11 The Crywolf Issue in Earthquake Early Warning Applications for the Campania Region

Iunio Iervolino[1], Vincenzo Convertito[2], Massimiliano Giorgio[3], Gaetano Manfredi[1], Aldo Zollo[4]

[1] Dipartimento di Analisi e Progettazione Strutturale, Università di Napoli Federico II, Naples, Italy
[2] RISSC-Lab, - Istituto Nazionale di Geofisica e Vulcanologia, Osservatorio Vesuviano, Naples, Italy
[3] Dipartimento di Ingegneria Aerospaziale e Meccanica, Seconda Università di Napoli, Aversa, Italy
[4] RISSC-Lab, Dipartimento di Scienze Fisiche, Università di Napoli Federico II, Naples, Italy

Abstract

Earthquake early warning systems (EEWS), based on real-time prediction of ground motion or structural response measures, may play a role in reducing vulnerability and/or exposure of buildings and lifelines. Indeed, seismologists have recently developed efficient methods for real-time estimation of an event's magnitude and location based on limited information of the P-waves. Therefore, when an event occurs, estimates of magnitude and source-to-site distance are available, and the prediction of the structural demand at the site may be performed by Probabilistic Seismic Hazard Analysis (PSHA) and then by Probabilistic Seismic Demand Analysis (PSDA) depending upon EEWS measures. Such an approach contains a higher level of information with respect to traditional seismic risk analysis and may be used for real-time risk management. However, this kind of prediction is performed in very uncertain conditions which may affect the effectiveness of the system and therefore have to be taken into due account. In the present study the performance of the EWWS under development in the Campania region (southern Italy) is assessed by simulation. The earthquake localization is formulated in a Voronoi cells approach, while a Bayesian method is used for magnitude estimation. Simulation has an empirical basis but requires no recorded signals. Our results, in terms of hazard analysis and false/missed alarm probabilities, lead us to conclude that the PSHA depending upon the EEWS significantly improves

seismic risk prediction at the site and is close to what could be produced if magnitude and distance were deterministically known.

11.1 Introduction

Seismic risk management consists of: (1) Risk mitigation by vulnerability or exposure reduction; (2) Emergency rapid response. Emergency preparedness is a near-real-time issue; risk mitigation strategies are typically mid-term (i.e. seismic retrofit of structures and infrastructures) or long-term actions (e.g. land use planning or development of appropriate design standards). An earthquake early warning and rapid response system can provide the critical information needed: (i) to minimize loss of lives and property, and (ii) to direct rescue operations (Wieland 2001). Therefore early warning systems may play a role in both of the risk management issues (Iervolino et al. 2007, this issue). In particular, in near-real-time applications shake maps, which are territorial distributions of ground shaking, are provided by a regional seismic network and already used for emergency management (Wald et al. 1999, Kanamori 2005, Convertito et al. 2007, this issue). On the other hand, seismic early warning systems are now capable of providing, from a few seconds to a few tens of seconds before the arrival of strong ground shaking, a prediction of the ground motion or the seismic demand on structures caused by a large earthquake. Therefore they may be used to take real time action for vulnerability or exposure reduction in the light of seismic risk management.

Earthquake early warning systems (EEWS) may simplistic be classified as *regional* or *site-specific*. Regional EEWS consist of wide seismic networks covering a portion of the area threatened by quake strike. Such systems are designed to provide real-time, or near-real-time information suitable for spreading the alarm to the community or inferring data (i.e. shake maps). Site-specific EEWS also enhance the safety margin of specific critical engineered systems such as nuclear power plants (Wieland 2000) or lifelines. The networks devoted to site specific EEW are much smaller than those of the regional type, only covering the surroundings of the system. The location of the sensors depends on the lead time needed to activate the safety procedures before the arrival of the more energetic seismic phase (i.e. S or superficial waves). Typically the alarm is issued when the ground motion at one or more sensors exceeds a given threshold; uncertainty, in this case, is often neglected since the path between the network and the site is limited.

Due to a large and rapid development of regional networks in recent years worldwide (see SAFER 2005 for example) the question of using EEWS for structure-specific applications is being raised (Iervolino et al. 2005). EEWS predictions may be used for the real time set-up of active or semi-active structural control, in order to achieve a safer structural response to ground motion. The "early" information provided by the regional EEWS in the first seconds of the event can be still used, in case of alarm, to activate different types of security measures, such as the shutdown of critical systems, evacuation of buildings, stopping of high speed trains (Veneziano and Papadimitriou 1998) and shut-off of valves in gas and oil pipelines.

Whether a structure-specific application of a regional EEWS is feasible is the topic of the study presented herein. In this case the ground motion Intensity Measure (IM) or the Engineering Demand Parameter (EDP) of interest has to be estimated far from the sensor network's recordings and cannot be measured at the site. A scheme of the *hybrid* application of a regional network for structure-specific earthquake early warning is shown in Fig. 11.1.

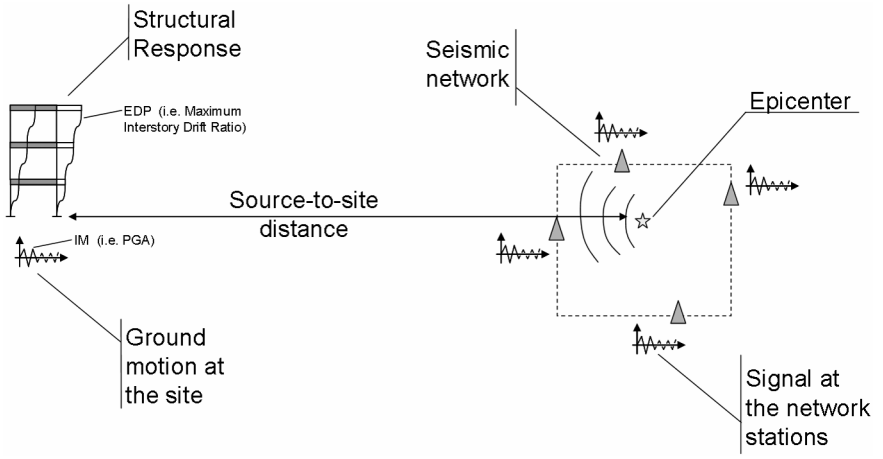

Fig. 11.1 Regional EWWS for structure-specific applications.

While the system captures the earthquake's features and then predicts IM and/or EDP at the site of interest to give additional lead time, this also

entails significant uncertainty[1] which may lead to false and missed alarms. Alerting or not alerting both have a cost; in the case of not alerting the loss is associated to an earthquake striking without any countermeasure being taken; in the case of alarm, preparing interventions has a cost (social and/or economic) which may transform into loss if the actual ground motion does not require such action. Therefore, a key issue in assessing EEWS performance is the estimation of missed and false alarm (MA and FA respectively) probabilities associated to the adopted decisional rule (Patè-Cornell 1986). Computation of MA and FA rates of occurrence on an empirical basis should consist of post-event analysis of EEWS predictions and would require a large strong-motion waveforms database both for the network and the site where the structure is located. Since such databases are very rarely available, especially for large earthquakes, the I and II type error probabilities related to MA and FA may be estimated in a simulation framework using appropriate characterizations of the uncertainties involved in the prediction. This approach requires virtually no records other than those used to calibrate the method adopted for the estimation of Magnitude (M) and source-to-site distance (R).

11.2 Seismic Risk Analysis Conditioned to the Earthquake Early Warning System

Recently seismologists have developed several methods to estimate an event's magnitude based on limited information of the P-waves (e.g. first few seconds of velocity recording) for real-time applications (Allen and Kanamori 2003). Similarly, as briefly described below, the source-to-site distance may be predicted by a sequence of network stations triggered by the developing earthquake (Satriano et al. 2007, this issue). Therefore, since it may be assumed that at a given instant estimates of M and R are available, the prediction of the ground motion at the site can be performed in analogy with Probabilistic Seismic Hazard Analysis (PSHA) (Cornell 1968, McGuire 1995). This results in a seismic hazard analysis conditioned (in a probabilistic sense) by the real-time information given by the EEWS. Consequently, the distribution of the structural response may also be computed by Probabilistic Seismic Demand Analysis or PSDA (Carballo and Cornell 2000, Cornell et al. 2002) provided there is an IM-EDP relationship for the structure of interest. It is easy to recognize that the

[1] It is worth noting that the site-specific EEWS reads IM directly while the regional predicts IM/EDP which is a more uncertain process.

probability density function of the structural response at the site when an event is occurring contains the highest level of information available and therefore is the best tool for real-time decision making.

11.2.1 EWWS-conditioned PSHA and PSDA

Let us assume that at a given time t from the earthquake's origin time, the seismic network can provide estimates of M and R. These probability density functions (PDFs) are intrinsically conditioned to a vector of measures, say $\{\tau_1, \tau_2, ..., \tau_\nu\}$ where ν is the number of instruments at which the measure of interest is available. Then the PDF of M has to be indicated as $f_{M|\tau_1,\tau_2,...,\tau_\nu}(m \mid \tau_1, \tau_2, ..., \tau_\nu)$; similarly the PDF of R, which for the method used only depends on the sequence of stations triggered, will be referred to as $f_{R|s_1,s_2,...,s_\nu}(r \mid s_1, s_2, ..., s_\nu)$ where $\{s_1, s_2, ..., s_\nu\}$ is such a sequence. Thus it is possible to compute the probabilistic distribution (or hazard curve) of a ground motion Intensity Measure (i.e. Peak Ground Acceleration or PGA) at the site, in analogy with the seismic hazard integral reported in Eq. (11.1), repeating it for several values of IM.

$$f_\nu(im) = \int_M \int_R f(im \mid m, r)\, f_{M|\tau_1,\tau_2,...,\tau_\nu}(m \mid \tau_1, \tau_2, ..., \tau_\nu) \\ f_{R|s_1,s_2,...,s_\nu}(r \mid s_1, s_2, ..., s_\nu)\, dr\, dm \quad im \in [0, +\infty] \tag{11.1}$$

where the PDF, $f(\text{im} \mid \text{m}, \text{r})$, is given by an attenuation relationship as in the ordinary PSHA. The subscript ν indicates that the computed hazard curve refers to a particular set of triggered stations and changes when a large amount of data is included in the process (e.g. more stations are triggered as time flows).

For structural applications of the EEWS the prediction of the structural response in terms of an Engineering Demand Parameter (EDP), rather than in terms of a ground motion IM, may be of prime concern. This requires a further integration to get the PDF of EDP as reported in Eq. (11.2).

$$f_\nu(edp) = \int_{IM} f(edp \mid im)\, f_\nu(im)\, dim \quad edp \in [0, +\infty] \tag{11.2}$$

where the PDF, $f(\text{edp} \mid \text{im})$, is the required probabilistic relationship between IM and EDP. If a Moment Resisting Frame (MRF) structure is concerned, for example, the PSDA procedure allows to obtain the relation ex-

pressed in Eq. (11.3) between the Maximum Inter-storey Drift Ratio (MIDR) and $Sa(T_1)$ (first mode spectral acceleration), which are the IM and EDP respectively.

$$MIDR = a\left(Sa(T_1)\right)^b \varepsilon \tag{11.3}$$

where the log of ε is a normal random variable with zero-mean and variance equal to the variance of the logs of MIDR, and the coefficients *a* and *b* are obtained via non-linear incremental dynamic analysis (Vamvakistos and Cornell 2000). Barroso and Winterstein (2002) have proposed a similar relationship for controlled structures.

For the sake of simplicity it will be assumed in the following that the parameter of interest is IM. This keeps the presentation of the method clear and ensures the results of the application are easier to interpret. Since EPD is only a probabilistic transformation of IM this choice does not affect the generality of the discussion.

11.2.2 Magnitude Estimate

The integral given in Eq. (11.1) requires the distribution of magnitude estimated on the basis of data provided by the network at a given time. Allen and Kanamori (2003) provide the relationship between the magnitude of the event and the log of the predominant period $\tau_{P,max}$ (simply τ herein) of the first four seconds of the P-waves for the TriNet network. It has been assumed that the distributions of τ, conditioned to the magnitude of the event $f_{\tau|M}(\tau \mid m)$, are lognormal. The mean of the logs and variance, retrieved from the data in the homoscedasticity hypothesis (Fontanella 2005), are reported in Eq. (11.4).

$$\begin{cases} \mu_{\log(\tau)} = \dfrac{(M - 5.9)}{7} \\ \sigma_{\log(\tau)} = 0.16 \end{cases}. \tag{11.4}$$

These distributions enable us to compute the estimation of magnitude, $f_{M|\tau_1,\tau_2,\ldots,\tau_v}(m \mid \tau_1, \tau_2, \ldots, \tau_v)$, using a Bayesian approach. In fact, if at a given time only one station is triggered measuring τ_1 from the first four seconds of the signal, the sought distribution of magnitude, conditioned to such measurement, $f_{M|\tau_1}(m \mid \tau_1)$, is the *posterior* of Eq. (11.5).

$$f_{M|\tau_1}\left(m \mid \tau_1\right) = \frac{f_{\tau_1|M}\left(\tau_1 \mid m\right) f_M\left(m\right)}{\int_{M_{MIN}}^{M_{MAX}} f_{\tau_1|M}\left(\tau_1 \mid m\right) f_M\left(m\right) dm} \tag{11.5}$$

where $\mathrm{f_M(M)}$ is the *a priori* PDF of the magnitude, Eq. (11.6), from the Gutenberg-Richter recurrence relationship and the denominator is the marginal distribution of τ, $\mathrm{f}_{\tau_1}\left(\tau_1\right)$.

$$f_M\left(m\right): \begin{cases} \dfrac{\beta e^{-\beta m}}{e^{-\beta M_{\min}} - e^{-\beta M_{\max}}} & M_{\min} \le m \le M_{\max} \\ 0 & m \notin \left[M_{\min}, M_{\max}\right] \end{cases}. \tag{11.6}$$

As time elapses, the number of stations which may be included in the magnitude estimation increases, new data are therefore available, and the posterior distribution may then be updated. At the time when a number ν of stations have measured τ, Eq. (11.5) can be generalized as Eq. (11.7).

$$f_{M|\tau_1,\tau_2,\ldots,\tau_\nu}\left(m \mid \tau_1,\tau_2,\ldots,\tau_\nu\right) = \frac{f_{\tau_1,\tau_2,\ldots,\tau_\nu|M}\left(\tau_1,\tau_2,\ldots,\tau_\nu \mid m\right) f_M\left(m\right)}{\int_{M_{MIN}}^{M_{MAX}} f_{\tau_1,\tau_2,\ldots,\tau_\nu|M}\left(\tau_1,\tau_2,\ldots,\tau_\nu \mid m\right) f_M\left(m\right) dm}. \tag{11.7}$$

Assuming that, conditionally upon M, the τ measurements are stochastically independent, then $\mathrm{f}_{\tau_1,\tau_2,\ldots,\tau_\nu|\mathrm{M}}\left(\tau_1,\tau_2,\ldots,\tau_\nu \mid \mathrm{m}\right) = \prod_{\mathrm{i}=1}^{\nu} \mathrm{f}_{\tau_\mathrm{i}}\left(\tau_\mathrm{i} \mid \mathrm{m}\right)$ which is the product of known terms. Therefore Eq. (11.7) may be rewritten as Eq. (11.8) which, applied for all the values of $m \in \left[M_{\min}, M_{\max}\right]$, gives the full magnitude PDF to be plugged into the PSHA integral.

$$f_{M|\tau_1,\tau_2,\ldots,\tau_\nu}\left(m \mid \tau_1,\tau_2,\ldots,\tau_\nu\right) = \frac{\left(\prod_{i=1}^{\nu} f_{\tau_i}\left(\tau_i \mid m\right)\right) f_M\left(m\right)}{\int_{M_{MIN}}^{M_{MAX}} \left(\prod_{i=1}^{\nu} f_{\tau_i}\left(\tau_i \mid m\right)\right) f_M\left(m\right) dm}. \tag{11.8}$$

It is possible to recognize that the distribution of magnitude (the same applies for distance) is indirectly dependent on time because, if at two different instants two different sets of triggered stations and measurements correspond, they will lead to two distributions of magnitude. Therefore the hazard integral in Eq. (11.1) may be re-computed at every time new stations perform measurements of τ. It will be shown in simulation how the

prediction improves with time as the number of triggered stations increases.

11.2.3 Real-time Location and Distance PDF

The real-time location methodology is that of Satriano et al. (2007, this issue) which is based on the equal differential-time formulation (EDT). For a detailed discussion the reader should refer to the above author's paper in this same book and only a brief description of the main features of the procedure are given in this section for readability purposes.

The hypocentral location technique follows an evolutionary and full probabilistic approach. It relies on the stacking of EDT surfaces; this is robust in respect to outlier data (e.g. wrong signal picking in the case of concurrent events). With just one recorded arrival, hypocentral position can be already constrained by the *Voronoi cell* associated to the triggered station. As time flows and more triggers become available, the evolutionary location converges to a standard EDT location.

The algorithm defines a dense grid of points (e.g. 1 km spaced) in the space below the network. At each time step, based only on the information on which stations are triggered and which are not yet triggered, it is possible to assign, to any the of the grid points, the probability of that point being the hypocenter. This leads to the definition of a time-dependent spatial PDF for the location. Therefore, at any time t, the distance estimate in terms of $f_{R|s_1,s_2,...,s_v}(r \mid s_1, s_2, ..., s_v)$ may be retrieved by a geometric transformation which associates to any particular distance a probability which is the sum of the probabilities of all points of the grid with the same distance to the site.

11.3 Decisional Rule, False and Missed Alarms

Once the EWWS provides a distribution of the ground motion intensity measure or seismic demand for the structure of interest, a decisional condition has to occur to issue the alarm. Several options are available to formulate a decisional rule, for example: (a) the alarm may be launched if the expected value $(E[IM])$ of the variable exceeds a threshold (IM_C); (b) alternatively, in a more sophisticated way, the alarm may be issued when the probability of the variable exceeding the threshold crosses a reference value (P_C). These decisional rules are given in Eqs. (11.9) and (11.10) respectively.

$$Alarm : E[IM] = \int_0^{+\infty} im \; f_\nu(im)\, dim > IM_C \tag{11.9}$$

$$Alarm : P[IM > IM_C] = 1 - \int_0^{IM_C} f_\nu(im)\, dim > P_C \,. \tag{11.10}$$

It is worth noting that the decisional rule (a) does not require the full computation of the hazard integral, Eq. (11.1). In fact, the expected value of IM may be well approximated by a First Order Second Moment (FOSM) method (Pinto et al. 2004), thereby reducing the computational effort. However, this decisional rule has the disadvantage of not considering the variance of IM nor the shape of its PDF. In the case of option (b) the P_C value has to be set in relation to an appropriate loss function. This second approach is more consistent with a full probabilistic approach to earthquake early warning for seismic risk management.

While performance of the early warning system may be tested to verify whether it correctly predicts the distribution of IM at the site, the efficiency of the decisional rule depends on I and II type errors which are related to the assessment of the false and missed alarm probabilities, P_{FA} and P_{MA} respectively[2]. Referring to Eqs. (11.9) and (11.10) the false alarm occurs when the EEWS issues the alarm while the intensity measure at the site IM_T (T subscript means "true" indicating the realization of the random variable to distinguish it from the prediction of the EEWS) is lower than the threshold IM_C. Probabilities of these events, Eq. (11.11), will be estimated in simulating (e.g. by a Montecarlo approach) the Campania EEWS for the decisional rules considered.

$$\begin{cases} Missed\ Alarm : \{no\ Alarm \cap IM_T > IM_C\} \\ False\ Alarm : \{Alarm \cap IM_T \le IM_C\} \end{cases}. \tag{11.11}$$

It has been discussed how the information and hence the uncertainty involved are dependent on the number of stations triggered at a certain time. Therefore, in principle, the decisional condition may be verified at any time from the triggering of the first station, and consequently the false and missed alarm probabilities are, also indirectly, a function of time. From this point of view the decisional process is again time-dependent, and one

[2] Of course the underlying hypothesis of EEWS is that it is more important to reduce missed alarms rather than false alarms, otherwise the system would be unnecessary.

may decide to alert when the trade-off between the available lead time and the losses related to a missed or false alarm is at its optimum.

11.4 Simulation of the SAMS Earthquake Early Warning System

The Campania early warning system (SAMS - Seismic Alert Management System) is based on the developing seismic network in the Apennines, spanning the regions of Campania and Basilicata (Weber et al. 2007, this issue). This network operates in the seismically most active area for Campania (100 km x 80 km wide) and is designed to acquire non-saturated data for earthquakes larger than 4 [M_w]. In Fig. 4.1 (see Chap. 4) the stations of the EW network (dark squares); the M > 2 events recorded from 1981 to 2002 and the faulting system of the Irpinia 1980 earthquake are given, showing how the network covers the most hazardous area in the region. Light squares represent additional stations which will be used to calibrate local attenuation relationships (Convertito et al. 2007, this issue).

To assess the performance of the EEWS on an empirical basis a large number of recordings should be available. In principle, to simulate the prediction of the IM at the site and comparing it with the actual value experienced by the structure, for any event, a set of recordings in each station and at the site should be available. However, it is possible to compute the false and missed alarm probabilities without data but still on an empirical basis by simulation (e.g. Montecarlo). The procedure has been implemented in a computer code and it takes advantage of empirical methods for the estimation of magnitude and distance calibrated by seismologists off-line.

Each run simulates a specific seismic event occurring in the area of interest and consists of three steps: (1) Simulation of the event's features (e.g. assignment of the event's magnitude; location and true IM at the site); (2) Simulation of the measurements and predictions (e.g. real-time PSHA) made by the network at any instant up to the triggering of all the stations; (3) Verification the decisional condition and of the false/missed alarm; (4) Count of the number of false/missed alarms to compute their frequency of occurrence. The flow chart of the simulation procedure is given in Fig. 11.2.

The site considered in the simulation is assumed to be in the city of Naples which is approximately 110km from the center of the network. In Fig. 11.3a the relative position of the network and the site are given as in the scheme in Fig. 11.1.

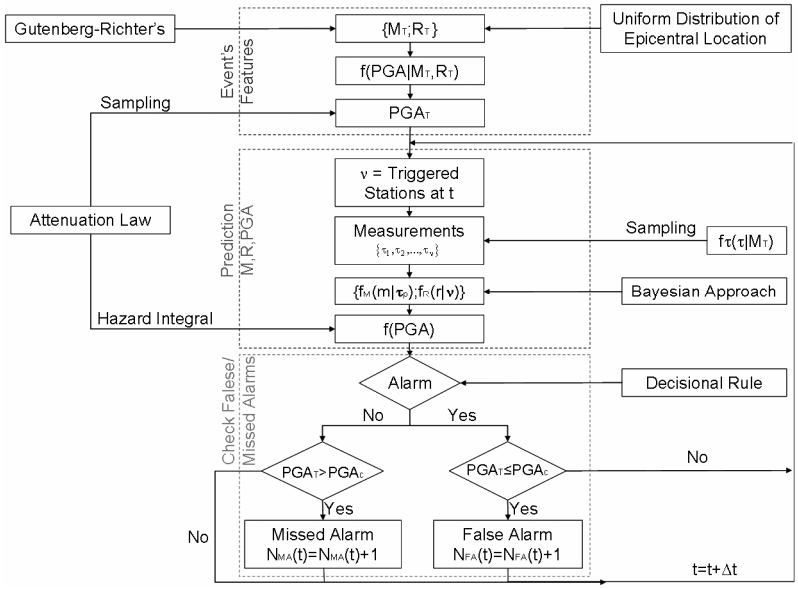

Fig. 11.2 Simulation flow chart.

11.4.1 Event and Ground Motion Feature Generation

Each run in the Montecarlo simulation starts with the generation of the geophysical features the EEWS will try to estimate. These values will completely define the earthquake of that run. In other words, since to compute the PSHA dependent on the EEW information the distributions of M and R are required, we need to establish the true value of those which will be called M_T and R_T (true magnitude and true source-to-site-distance respectively). Moreover, the ground motion intensity measure at the site (IM_T) has to be fixed; it is needed to verify the decisional condition and see whether a false or missed alarm has occurred.

The true magnitude of the event (M_T) may be sampled according to the Gutenberg-Richter recurrence relationship for the Campania region [in Eq. (11.6); $\beta = 1.69$, $M_{min} = 4$, $M_{max} = 7$]. On the other hand, one may be interested in evaluation the EEWS performance with respect to a specific magnitude; hence M_T for the all runs in the simulation has to be set at the same value. This is useful in the light of assessing the EEWS's perform-

ance in the case of high magnitude events which are the most threatening. Below, this second option will be followed for sake of clarity and readability of results.

The location of the epicenter is randomly chosen by sampling its coordinates $\{x_{epi}, y_{epi}\}$ from two s-independent uniform distributions defined in the area covered by the network. Once the epicentral coordinates are set the distance R_T to the site of interest (e.g. Naples) is readily obtained. (In Fig. 11.3b the simulated event locations in 1000 runs are given.) Again, for some purposes one may want to set the location of the epicenter at the same point for all the simulations. Therefore, in this case, the value of R_T is fixed for all the simulations.

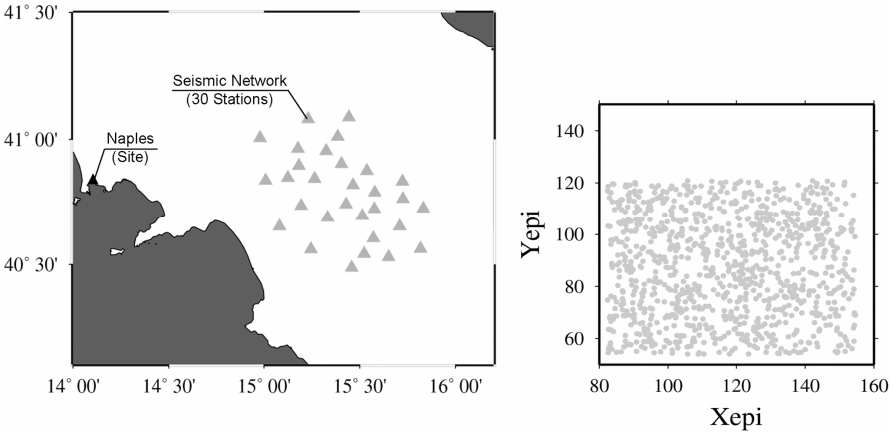

(a) (b)

Fig. 11.3 The EEWS-site Campania scheme (**a**); the sampled epicentral locations in 1000 runs (**b**).

The generation (or assignment) of a "true" magnitude and "true" distance in each Montecarlo run allows us to get reference values for the prediction of the EEWS. However, the "true" ground motion at the site (IM_T) should also be set. It is required to verify the decisional condition: for example, it has to be compared to the expected value of IM computed by the EEWS, Eq. (11.9), to establish whether the decision adopted produced, in that run, a missed or false alarm. The value of IM_T at the site, consistent with the values of M_T and R_T, is obtained by sampling the attenuation relationship which, by definition, provides the PDF of the ground motion in-

tensity measure conditioned to $\{M_T, R_T\}$. Herein the Sabetta and Pugliese (1996) attenuation is considered in its epicentral formulation to be consistent with the location estimation method. The considered IM is the PGA; hence, in each run the value of PGA_T is sampled from a completely specified lognormal random variable[3].

Finally the event is completely defined for EEWS purposes since $\{M_T, R_T, PGA_T\}$ of the generic run are set; the next step consists in simulating the measurements at the stations consistently with the event's features.

11.4.2 Station Measurements and M,R Real-time Distributions

In the simulation process, at any given time, the number of stations triggered is computed. This is carried out assuming a homogeneous and isotropic propagation model with P- and S-waves velocities of 5.5km/s (V_P) and 3.5km/s (V_S) respectively. This allows, for any epicentral location, determination of which stations are triggered at any time. Similarly the lead time, defined as the time required for the S-waves to hit the site, may be computed at each instant of time.

Once the event is defined by $\{M_T, R_T, PGA_T\}$, the response and predictions of the seismic network should be simulated (e.g. the measurement of τ) without any recording but consistently with the measures that would be performed in the real case. For example, let first consider the case when only one station is triggered[4]. It is possible to simulate the station's measurement by sampling the empirical distribution of the parameter to be measured conditioned to the true magnitude of the event, $f_{\tau|M}(\tau \mid M_T)$. Real τ values measured from recorded signals would be distributed as $f_{\tau|M}(\tau \mid M_T)$ by definition, and therefore such sampling is appropriate in a simulation approach.

To generate τ for more than one station it is assumed that measurements performed by different stations are s-independent conditionally upon the event's magnitude (M_T). Therefore, at a given time t when ν stations are triggered, all the ν component of the $\{\tau_1, \tau_2, ..., \tau_\nu\}$ vector are obtained by

[3] If many recorded signals were available at the site for a given magnitude, the empirical distribution of the IM as retrieved by the records should be the same as that provided by the attenuation law.

[4] Again, due to the magnitude estimation method adopted, four seconds have to elapse after the triggering of the station to include it in the estimation process.

sampling ν times the same $f_{\tau|M}(\tau \mid M_T)$ PDF. Since data by Allen and Kanamori (2003) are based on τ measurements on four seconds of recording, herein the working hypothesis is that any station's measurement is considered in the process if four seconds have elapsed from its triggering. Moreover, no evolution in time of the τ measure is considered.

Once the measurement vector $\{\tau_1, \tau_2, ..., \tau_\nu\}$ is available, the Bayesian method of section 2.2 may be applied to compute the distribution of magnitude. In Fig. 11.4 the resulting magnitude distributions for a simulated M 6 event are given, clearly showing that, when few stations are triggered, the distributions underestimate the magnitude.

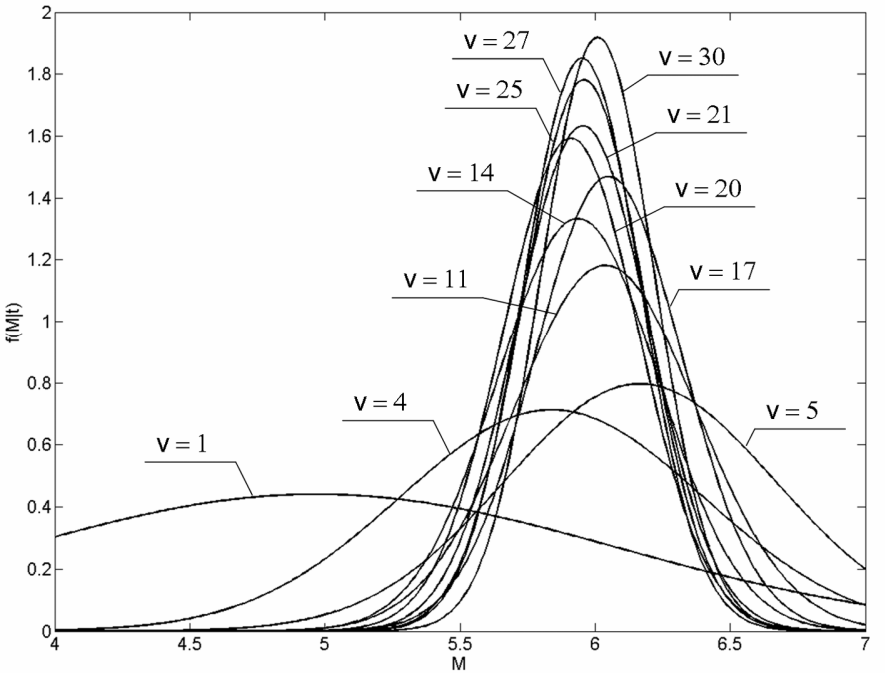

Fig. 11.4 Magnitude distribution as the number of triggered stations increases ($M_T = 6$, $R_T = 91$km).

Indeed, when few data are available, the dominating information is that *a priori* of Eq. (11.6) which naturally tends to give larger occurrence probability to low magnitude events. More precisely, the Bayesian approach will tend to produce overestimates of magnitude when it is below the *a priori* mean and it will tend to underestimate it when it is greater than the

mean. This effect is directly proportional to the difference in the expected value of the *a priori* and M_T and inversely proportional to the size of measurement vector. Then, as more measurements became available, the prediction centers on the real value with a relatively small uncertainty. An estimator with these features is said to be biased by classic statisticians and other methods can be considered to obtain an unbiased estimator (i.e. maximum likelihood). However, the Bayesian approach was preferred since, albeit slightly biased, it gives, on average, significantly smaller estimation errors due to the use of the *a priori* information.

A similar observation applies to the distribution of the source-to-site distance. As earthquake location is only dependent on the sequence of stations triggered, no measurements have to be simulated to compute $f_{R|S_1,S_2,...,S_v}(r|S_1,S_2,...,S_v)$ once the arrival time ($t_{a,j} = R_j/V_P$ where R_j is the distance of the j-th station from the epicenter) has been computed for all the stations in the network.

The estimation process for the magnitude starts four seconds after the triggering of the first station. At that time it is assumed that the location (and therefore the distance) is known. This is not a limiting hypothesis: simulations show that the localization method after a few seconds (e.g. 3s) reduces the uncertainty on the location to about 1 km, which is negligible in respect to other uncertainties involved in the process.

11.4.3 Seismic Risk Analysis

The estimated distributions of M and R, along with the attenuation law, in the hazard integral allow us to compute the exceeding probability of PGA at the site as the event evolves and the stations trigger. The hazard curves corresponding to the event simulated in Fig. 11.4 are given in Fig. 11.5. It is possible to see the evolution of hazard which stabilizes when a large number of stations provide information about the τ measurements.

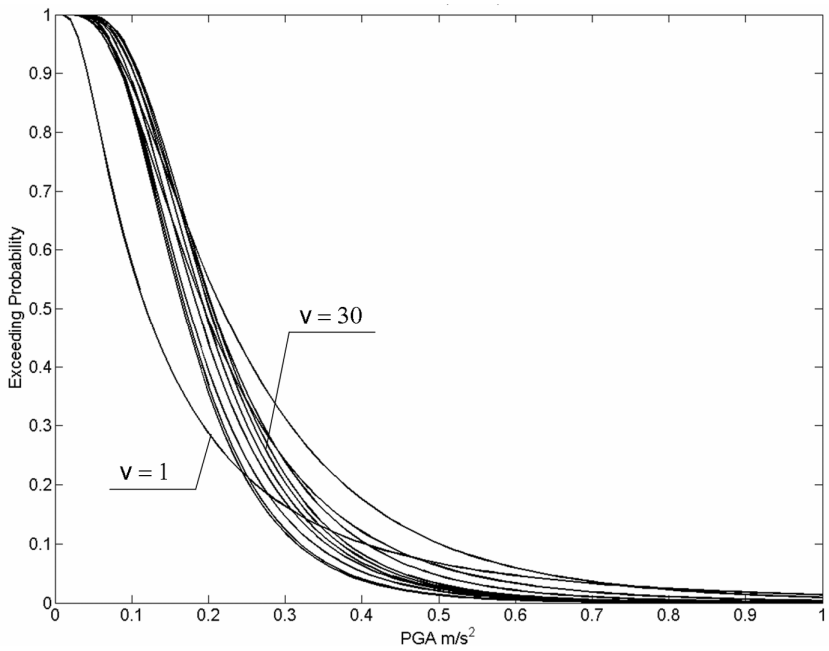

Fig. 11.5 EWWS-conditioned seismic hazard as the number of stations increases ($M_T = 6$, $R_T = 91$km).

To better understand whether the hazard computed with EEWS information is correct, it is worth comparing it to the "maximum knowledge status" of the hazard by adopting the true value of magnitude and distance (as if they were deterministically known). This corresponds to the exceeding probability of PGA when M and R are fixed. This comparison is shown in Fig. 11.6: a thick curve represents the complementary Cumulative Density Function (CDF) for the PGA when M_T (7) and R_T (110km) are known; the black curves are the results of 200 simulations. (In the figure only the hazard curves corresponding to the case when all stations triggered ($\nu = 30$) are reported.) The EEWS hazard may be seen to correctly approximate the maximum knowledge condition.

To reduce the variability of the hazard curves, a strategy would be to increase the number of stations. Indeed, the estimation procedure of the magnitude distribution would benefit from the larger vector of information.

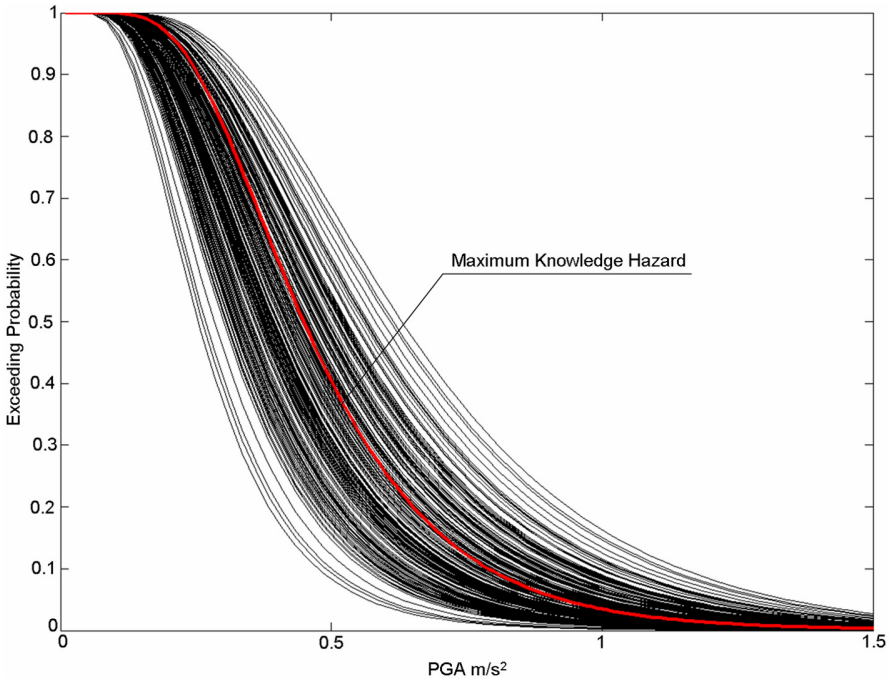

Fig. 11.6 EWWS-conditioned seismic hazard in 200 simulations compared to the maximum knowledge condition ($M_T = 7,\ R_T = 110$km).

11.4.4 False and Missed Alarm Probabilities

The simulation (Fig. 11.2) also allows the frequency of false and missed alarms, Eq. (11.11), to be computed according to the decisional rule chosen. For example, according to Eq. (11.9) these probabilities are estimated as in Eq. (11.12).

$$\begin{cases} P_{MA} \cong \dfrac{N\left[E\left[PGA\right] \le PGA_C \cap PGA_T > PGA_C\right]}{N_{TOT}} \\ P_{FA} \cong \dfrac{N\left[E\left[PGA\right] > PGA_C \cap PGA_T \le PGA_C\right]}{N_{TOT}} \end{cases} \tag{11.12}$$

where N is the number of occurrences of MA or FA and N_{TOT} is the number of simulated events. Analogously, for the decisional rule of Eq. (11.10) the probabilities are estimated as in Eq. (11.13).

$$\begin{cases} P_{MA} \cong \dfrac{N\left[P\left[PGA > PGA_C\right] \le P_C \cap PGA_T > PGA_C\right]}{N_{TOT}} \\ P_{FA} \cong \dfrac{N\left[P\left[PGA > PGA_C\right] > P_C \cap PGA_T \le PGA_C\right]}{N_{TOT}} \end{cases}. \tag{11.13}$$

In Fig. 11.7 such estimations are given for M 7 (10^4 simulations) events with an epicentral distance of 110km. The PGA_C is arbitrarily set at 0.3m/s^2 and the critical probability of exceedance (P_C) is 0.2.

The real-time PSHA is performed at each second from the nucleation of the event and hence a prediction of the PGA at the site is evolving with time. Consequently; the false and missed alarm occurrence also changes with time, which has implications for the risk management strategy. For example, since the false alarm probability is decreasing for all decisional rules, alerting at a certain time means accepting some greater error probability than if the alarm were issued later, although this implies additional lead time.

To better understand the results of Fig. 11.7 it is useful to discuss the given curves. In particular we will focus on the decisional rule of Eq. (11.10). The critical value of PGA (PGA_C) is 0.3m/s^2, the true value of magnitude and distance are M_T = 7 and R_T = 110km respectively. The chosen attenuation relationship, conditioned by M_T and R_T, gives $P\left[PGA > PGA_C\right]$ = 0.81. Hence if P_C is equal to 0.2, the right decision would be to alert at every run. As a consequence, the probability of a missed alarm is zero because the alarm should always be issued and the probability of a false alarm is $P\left[PGA \le PGA_C\right]$ or 1-0.81 = 0.19. These probabilities are intrinsic to the decisional rule and the thresholds set. However, as discussed, the EEWS cannot perfectly estimate the hazard curve with M_T and R_T known (thick curve). In fact, due to the variability in the estimated hazard, the value $P\left[PGA > PGA_C\right]$ is sometimes underestimated and sometimes overestimated. For example the underestimation of $P\left[PGA > PGA_C\right]$ leads to the alarm not being given even if required and therefore the missed alarm curve is not zero. In particular, when there are few triggered stations this underestimation effect is strong and the missed alarm probability is relatively high because when the alarm is not launched (incorrectly) it will most likely result is a missed alarm. As time elapses, the estimation improves, $P\left[PGA > PGA_C\right]$ tends to its correct value (0.81) and the missed alarm probability also tends to its correct value (0). On the

other hand the false alarm tends to 0.19. This means that, when all stations are triggered, the systems will work according to what has been designed.

The shape of the curves depends on both the chosen values of PGA_C and P_C and may thus be very different from those discussed in this example if other values of the thresholds are concerned. Nevertheless, given the missed and false alarm reference values calculated by means of the hazard conditioned by M_T and R_T, the system may be calibrated by setting PGA_C and P_C appropriately.

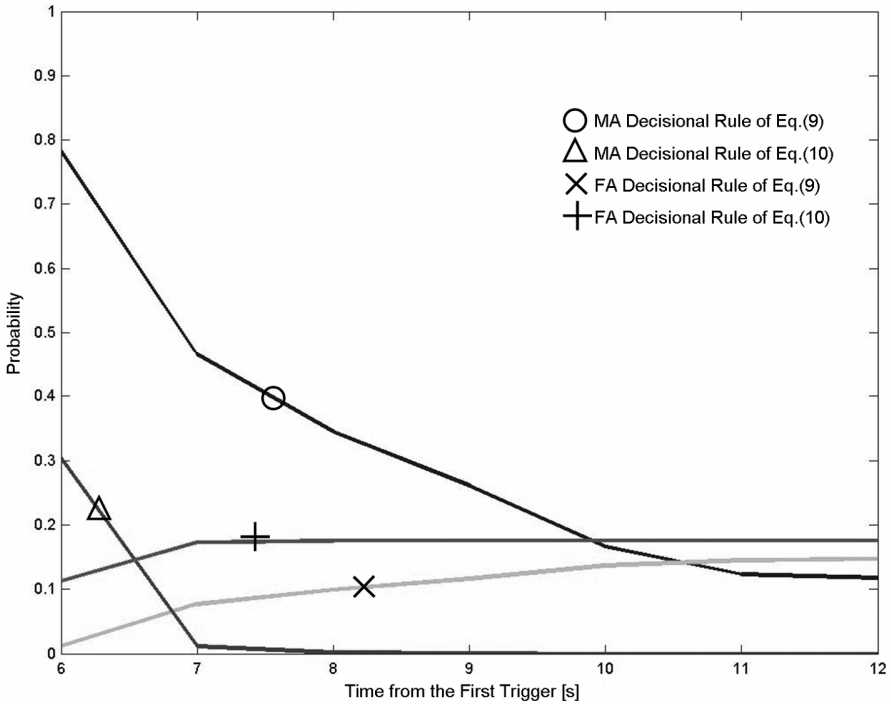

Fig. 11.7 False and missed alarm probabilities for 10^4 events ($M_T = 7$, $R_T = 110\text{km}$, $PGA_C = 0.3\text{m}/\text{s}^2$).

11.5 Conclusions

The discussed method aims to assess whether it is possible to use real-time information provided by an EEWS to estimate the seismic performance of

a structural or infrastructural system of interest. Magnitude and source-to-site distance probabilistic distributions are plugged into the hazard analysis, which may be further processed to obtain a prediction of the structural response for the event occurring. Real-time seismic risk analysis seems the way to use all the information provided by the earthquake early warning system for real-time decision making. However, since the site is most likely far from the network, the uncertainty related to the prediction cannot be neglected.

The approach was tested by simulating the Campania early warning system. Results indicate that the PSHA, conditioned to the EEWS measures, correctly approximates the hazard computed if the magnitude and distance were deterministically known, which is the maximum level of knowledge possible. A significant reduction in the dispersion of the hazard curves would be obtained by increasing the number of sensors in the area.

The approach is also used to test possible decisional rules to issue the alarm. Decisional rules and alarm thresholds have intrinsic (by design) missed and false alarm probabilities which may be changed according to appropriate loss functions. Simulation shows how the missed and false alarm probabilities estimated by the EEWS are evolving with time, approaching their design values as the number of stations increases. Such curves may be used for risk management, optimizing the trade-off between the probability of wrong decisions and the available lead time for risk reduction action.

11.6 Acknowledgements

The study presented in this paper was developed in the framework of the P.O.R. Campania 2000 - 2006, Misura 1, founded by the Campania Regional Authority. The authors are also grateful to Professor Daniele Veneziano (Massachusetts Institute of Technology) for his helpful discussions on the topic.

References

Allen RM, Kanamori H (2003) The Potential for Earthquake Early Warning in Southern California. Science 300:786-789

Barroso LR, Winterstein S (2002) Probabilistic Seismic demand analysis of controlled steel moment-resisting frame structures. Earthquake Engineering and Structural Dynamics 31:2049-2066

Carballo JE, Cornell CA (2000) Probabilistic Seismic Demand Analysis: Spectrum Matching and Design. Department of Civil and Environmental Engineering, Stanford University. Report No. RMS-41

Convertito V, De Matteis R, Romeo A, Zollo A, Iannaccone G (2007) A strong motion attenuation relation for early-warning application in the Campania region (Southern Apennines). In: Gasparini P, Manfredi G, Zschau J (eds) Earthquake Early Warning. Springer

Cornell CA (1968) Engineering seismic risk analysis. Bull Seismol Soc Am 58:1583-1606

Cornell CA, Jalayer F, Hamburger RO, Foutch DA (2002) The Probabilistic Basis for the 2000 SAC/FEMA Steel Moment Frame Guidelines. J of Struct Eng 128(4):526-533

Fontanella N (2005) Gestione del Rischio Sismico nella Regione Campania: Formulazione e Calibrazione del Simulatore del Sistema di Early Warning Sismico per il Progetto SAMS, MSc. Thesis, University of Naples Federico II. Advisors: M. Giorgio, I. Iervolino, V. Convertito (in Italian)

Iervolino I, Convertito V, Manfredi G, Zollo A, Giorgio M, Pulcini G (2005) Ongoing Development of a Seismic Alert Management System for the Campanian Region. Part II: The cry wolf issue in seismic early warning applications, Earthquake Early Warning Workshop, Caltech, Pasadena, CA [http://www.seismolab.caltech.edu/early.html]

Iervolino I, Manfredi G, Cosenza E (2007) Earthquake early warning and engineering application prospects. In: Gasparini P, Manfredi G, Zschau J (eds) Earthquake Early Warning. Springer

Kanamori H (2005) Real-time seismology and earthquake damage mitigation. Annual Review of Earth and Planetary Sciences 33:5.1-5.20

McGuire RK (1995) Probabilistic seismic hazard analysis and design earthquakes: Closing the loop. Bulletin of the Seismological Society of America 85:1275-1284

Pate-Cornell ME (1986) Warning systems in risk management. Risk Management 6:223-234

Weber E, Iannaccone G, Zollo A, Bobbio A, Cantore L, Corciulo M, Convertito V, Di Crosta M, Elia L, Emolo A, Martino C, Romeo A, Satriano C (2007) Development and testing of an advanced monitoring infrastructure (ISNet) for seismic early-warning applications in the Campania region of southern Italy. In: Gasparini P, Manfredi G, Zschau J (eds) Earthquake Early Warning. Springer

Pinto PE, Giannini R, Franchin P (2004) Seismic reliability analysis of structures. IUSSPress, Pavia, Italy

Sabetta F, Pugliese A (1996) Estimation of response spectra and simulation of nonstationarity earthquake ground motion. Bulletin of the Seismological Society of America 86:337-352

Satriano C, Lomax A, Zollo A (2007) Optimal, real-time earthquake location for early warning. In: Gasparini P, Manfredi G, Zschau J (eds) Earthquake Early Warning. Springer

Seismic eArly warning For EuRope – Safer (2005) Sixth Framework Programme Call: Fp6-2005-Global-4 Sustainable Development, Global Change and Ecosystem Priority 6.3.IV.2.1: Reduction of seismic risks

Vamvatsikos D, Cornell CA (2002) Incremental Dynamic Analysis. Earthquake Engineering and Structural Dynamics 31(3):491-514

Veneziano D, Papadimitriou AG (1998) Optimization of the Seismic Early Warning System for the Tohoku Shinkansen. 11th European Conference on Earthquake Engineering. Paris, France

Wieland M (2001) Earthquake Alarm, Rapid Response, and Early Warning Systems: Low Cost Systems for Seismic Risk Reduction. Electrowatt Engineering Ltd. Zurich, Switzerland

Wald DJ, Quitoriano V, Heaton TH, Kanamori H, Scrivner CW, Worden BC (1999) TriNet "ShakeMaps": Rapid Generation of Peak Ground Motion and Intensity Maps for Earthquake in Southern California. Earthquake Spectra 15:537-555

Wieland M, Griesser M, Kuendig C (2000) Seismic Early Warning System for a Nuclear Power Plant. Proc. of 12th World Conference on Earthquake Engineering. Auckland, New Zealand